Biosensors and Bioelectronics 49 (2013) 499–505

Contents lists available at SciVerse ScienceDirect

Biosensors and Bioelectronics

journal homepage: www.elsevier.com/locate/bios

A FRET ratiometric fluorescence sensing system for mercury detection and intracellular colorimetric imaging in live Hela cells

Bo Hu, Lin-Lin Hu, Ming-Li Chen *, Jian-Hua Wang *

Research Center for Analytical Sciences, Northeastern University, Box 332, Shenyang 110819, China

ARTICLE INFO

Article history:
Received 10 April 2013
Received in revised form
3 June 2013
Accepted 4 June 2013
Available online 12 June 2013

Keywords:
Quantum dots
Rhodamine 6G derivative
Fluorescence resonance energy transfer
Mercury sensing
Colorimetric imaging
Intracellular mercury

ABSTRACT

The detection of mercury in biological systems and its imaging is of highly importance. In this work, a ratiometric fluorescence sensor is developed based on fluorescence resonance energy transfer (FRET) with N-acetyl-L-cysteine functionalized quantum dots (NAC-QDs) as donor and Rhodamine 6G derivative-mercury conjugate (R6G-D-Hg) as acceptor. Mercury annihilates the fluorescence of NAC-QDs at 508 nm and meanwhile interacts with R6G derivative to form a fluorescent conjugate giving rise to emission at 554 nm. Resonance energy transfer from NAC-QDs to R6G-D-Hg is triggered by mercury resulting in concentration-dependent variation of fluorescence ratio F_{508}/F_{554}. A linear calibration of F_{508}/F_{554} versus mercury concentration is obtained within 5–250 μg L^{-1}, along with a detection limit of 0.75 μg L^{-1} and a RSD of 3.2% (175 μg L^{-1}). The sensor generates colorimetric images for mercury within 0–250 μg L^{-1}, facilitating visual detection of mercury with a distinguishing ability of 50 μg L^{-1}. This feature is further demonstrated by colorimetric imaging of intracellular mercury. On the other hand, the NAC-QDs/R6G-D FRET sensing system is characterized by a combination of high sensitivity and selectivity. The present study provides an approach for further development of ratiometric sensors dedicated to selective *in vitro* or *in vivo* sensing some species of biologically interest.

1. Introduction

Mercury is highly toxic for its bio-accumulative and persistent character (Han et al., 2010; Zahir et al., 2005; Boening, 2000; Tchounwou et al., 2003), which causes serious damage to the central nervous and endocrine systems (Boening, 2000; Mutter et al., 2005; Zahir et al., 2005; Magos and Clarkson, 2006). Mercury monitoring in various sample matrixes, especially in biological systems including human body, has been an important issue (Tang et al., 2008; Shamsipur et al., 2005). Quantification of mercury and its species in environment and living organisms is usually performed by bulky instrumentations, e.g., inductively coupled plasma mass spectrometry (ICP-MS) (Leermakers et al., 2005), atomic fluorescence spectrometry (AFS) (da Silva et al., 2013; Geng et al., 2008; Leopolda et al., 2008), atomic absorption spectrometry (AAS) (Erxleben and Ruzicka, 2005; Pourreza and Ghanemi, 2009) and high performance liquid chromatography with detection by ICP-MS or AFS (Hight and Cheng, 2006; Yin et al., 2007). These techniques provide low detection limit and are suitable for monitoring ultratrace mercury, however, their running is costly and complicated/tedious sample preparation procedures are often required (Yang et al., 2011; Kim et al., 2011). On the other hand, it is especially not suitable for *in vivo* or *in vitro* monitoring of intracellular mercury. In this respect, it is highly desirable to develop facile, economical and rapid methodologies with favorable sensitivity and selectivity for real time mercury sensing in biological samples or in human bodies (Darbha et al., 2007).

Molecular fluorescence is promising in biological and analytical sciences for mercury detection (Nolan and Lippard, 2008), among which fluorescence resonance energy transfer (FRET) has gained extensive attentions and exhibits favorable sensitivity and selectivity (Fang et al., 2008). FRET is able to derive ratiometric fluorescence for mercury sensing, and such procedures may eliminate fluorescence fluctuations arising from the instrument and experimental parameters, by performing measurement at two wavelengths to exclude spurious factors (Childress et al., 2012). This makes it feasible for colorimetric visual identification of mercury (Hu et al., 2012). However, so far very few FRET ratiometric fluorescence sensing procedures are available for mercury and thus further in-depth studies are required (Nolan and Lippard, 2008). FRET ratiometric fluorescence approaches generally require the donor to have sufficient long lifetime for eliminating interferences from short-lived background fluorescence and spectral overlap of donor emission and acceptor absorption. Quantum dots (QDs) are suitable donors in FRET systems attributed to their distinct properties, e.g., high quantum yields, photo-stability, tunable color with narrow emission bands and long fluorescent

* Corresponding authors. Tel.: +862483688944; fax: +862483676698.
E-mail addresses: chenml@mail.neu.edu.cn (M.-L. Chen), jianhuajrz@mail.neu.edu.cn (J.-H. Wang).

0956-5663/$ - see front matter © 2013 Elsevier B.V. All rights reserved.
http://dx.doi.org/10.1016/j.bios.2013.06.004

lifetime (Ma et al., 2005; Tsay et al., 2007). In addition, surface defects and Cd–S bonds between the stabilizers and QDs offer extra sensitivity to thiophile mercury (Duan et al., 2011). However, the selectivity of QDs so far reported is poor and interferences from sample matrixes frequently deteriorate applications for real samples (Pei et al., 2012).

As metal-responsive dyes (Dujols et al., 1997; Nguyen and Francis, 2003; Kwon et al., 2005), Rhodamine derivatives exhibit high selectivity toward spirolactam (non-fluorescent) structure, and have been employed for turn-on fluorescence sensing (Xiang and Tong, 2006; Kenmoku et al., 2007; Swamy et al., 2008; Kim et al., 2008; Chatterjee et al., 2009; Li et al., 2009; Li et al., 2010). The modification of Rhodamine B, Rhodamine 6G and Rhodamine 123 with small organic molecules results in non-fluorescent spirolactam or analogous structure due to the closed spirolactam ring (Wang et al., 2012). While the introduction of oxytropic or thiophilic metals promotes ring-opening reaction and gives rise to fluorescent conjugate (Yang et al., 2005). A Rhodamine 6G derivative with spirolactam structure was derived when Rhodamine 6G reacts with phenyl-iso-thiocyanate, revealing much improved selectivity to mercury. It should be addressed that the sensitivity of Rhodamine derivatives hitherto described is not feasible for practical applications in biological systems.

As discussed above, a new sensing system is expected to possess both high sensitivity and selectivity by combining advantages of QDs and Rhodamine derivatives. In this work, a novel FRET ratiometric fluorescence approach is developed with N-acetyl-L-cysteine stabilized QDs (NAC-QDs) as donor and R6G-D-Hg conjugate as acceptor. In mercury detection or imaging, the NAC-QDs/R6G-D FRET sensing system possesses both favorable sensitivity and selectivity. The sensing system also facilitates *in vitro* colorimetric imaging of mercury in live Hela cells.

2. Experimental section

2.1. Instrumentations and reagents

Fluorescence spectra are measured on an F-7000 fluorescence spectrophotometer (Hitachi Ltd., Japan) under excitation at 490 nm with a 700 V xenon discharge lamp as light source. Absorption spectra are recorded on a U-3900 UV–vis spectrophotometer (Hitachi Ltd., Japan) with a 1.0-cm quartz cell and a bandwidth setting of 1 nm at a scanning speed of 1200 nm min^{-1}. FT-IR spectra are obtained by using a Nicolet-6700 FT-IR spectrometer (Thermo Ltd., USA) within a range of 4000–500 cm^{-1}. ^1H NMR spectra is recorded on a Bruker ARX-600 spectrometer operated at 600 MHz. A UA-A portable dark-box ultraviolet analyzer (Shanghai JiaPeng Technology Co., Ltd., China) with excitation at 365 nm and a Canon SX210 IS camera are used for recording the fluorescence chromatic difference image of mercury. Hela cell images after uptaking the sensing materials (NAC-QDs/R6G-D) are recorded on an inverted fluorescent microscope (Nikon, Japan). The other equipments used include IKA vortex 3 (IKA Ltd., China), SW-CJ-1FD air clean bench (Antai Air Tech Co., Ltd., Suzhou, China), and LDZX-40BI stainless steel vertical pressure steam sterilizer (Shenan Medical Devices, Shanghai, China). Rhodamine 6G (R6G) is obtained from Beijing Biotopped Science & Technology Co., Ltd. (Beijing, China) and used without further purification. Phenyl-iso-thiocyanate, hydrazine hydrate (85%), N-acetyl-L-cysteine (NAC, AR), tellurium powder (AR), sodium tetrahydroborate ($NaBH_4$, 96%) and cadmium chloride ($CdCl_2 \cdot 2.5H_2O$, AR) are purchased from Sinopharm Chemical Reagent Co., Ltd. (Shanghai, China). Mercuric acetate ($(CH_3COO)_2Hg$, 99%, AR) is obtained from Xiya Chemical Reagent Co., Ltd. (Chengdu, China).

Phosphate buffer is obtained by mixing appropriate amount of 0.2 mol L^{-1} Na_2HPO_4 and NaH_2PO_4 solutions, and the pH value of the buffer is regulated with an Orion 818 pH meter (Thermo Fisher Scientific, USA). Deionized (DI) water of 18 MΩ·cm is used throughout the experiments.

2.2. Sample and sample pretreatment

Certified reference material (trace elements in city waste incineration ash, CRM 176): 0.0547 g of CRM 176 is taken into a PTFE digestion vessel along with a mixture of 3.0 mL HNO_3 (65%, w/v), 2.0 mL HCl (36%, w/v) and 0.5 mL HF (40%, w/v). After soaking for 2 h, the mixture is digested on a microwave oven with the following program: 150 °C/10 atm for 4 min, 170 °C/15 atm for 3 min, 190 °C/22 atm for 3 min and 210 °C/30 atm for 5 min. The reaction mixture in the digestion vessel is diluted with DI water to 10 mL for future use. A blank solution is processed by following the same process in the absence of target analyte.

Spring water (from GuanMen Moutain spring, Benxi, China), underground water (from HuShan Great Wall, Dandong, China) and polluted water (from Northern Shenyang Wastewater Treatment Plant, Shenyang, China) are collected for the purpose of demonstration of the developed procedure. In practice, the water samples are filtered through a 0.22 μm membrane filter and adjusted to pH 7 before analysis.

2.3. Preparation of NAC-stabilized quantum dots and Rhodamine 6G derivative

With N-acetyl-L-cysteine (NAC) as the stabilizer, the quantum dots (NAC-QDs) are prepared as shortly described herein: NaHTe solution is achieved by reducing Te powder with $NaBH_4$ at 0 °C for 3 h and then mixed with $CdCl_2$ solution under argon protection and refluxing at 96 °C (Zhao et al., 2010; Cao et al., 2010). By controlling the heating time for 1.5 h, NAC-QDs with green emission at ~510 nm are obtained. The NAC-QDs are then purified with isopropyl alcohol (QDs/isopropyl alcohol = 1:2, v/v) under centrifugation at 8000 rpm for 5 min then freeze-dried and re-dispersed in phosphate buffer (10 mmol L^{-1}, pH 7) for future use. The NAC-QDs are characterized by FT-IR spectra as illustrated in Supporting Information as Fig. S1, and pertinent descriptions are given therein.

Rhodamine 6G derivative (R6G-D) is prepared by a classical two-step approach using a literature procedure with modification as illustrated in Scheme S1 (Yang et al., 2005; Xiang et al., 2006). 5.0 mL of hydrazine monohydrate (85%) is added into a 25 mL Rhodamine 6G (1.2 g)-ethanol solution at room temperature under vigorous stirring and refluxing for 6 h to produce a precipitate. The reaction mixture is allowed to stand for overnight followed by washing the precipitate with ethanol and water alternatively for 3 times. After drying in vacuum, pale pink Rhodamine 6G hydrazine is collected.

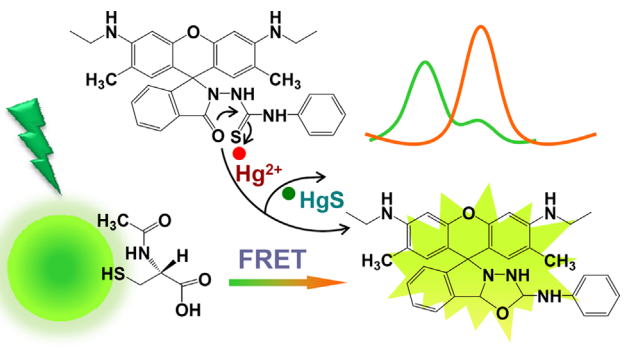

Scheme 1. The schematic illustration for mercury sensing based on the NAC-QDs/R6G-D-Hg FRET ratiometric fluorescence system .

0.06 g of the Rhodamine 6G hydrazine is dissolved in 12.0 mL of boiling methanol to react with 70 μL of phenyl-iso-thiocyanate for 2 h for producing white Rhodamine 6G derivative. After washing with 10 mL of cold methanol and drying under vacuum, 0.06 g of Rhodamine 6G derivative is collected, corresponding to a yield of 76.7%. The Rhodamine 6G derivative is characterized by ^{1}H NMR spectra as illustrated in Supporting Information as Fig. S2 showed with full chemical shift values.

2.4. Detection of mercury

NAC-QDs are used as donor while the conjugate between R6G-D and mercury is used as acceptor. In practice, R6G-D and mercury are mixed first to form R6G-D-Hg fluorescent conjugate. Afterward, NAC-QDs are added to construct the FRET sensing system. As shown in Fig. S3, the response of the sensing system closely related to the amount of R6G-D, and in the present study 0.066 mg is used. A reaction time of 5 min is employed to ensure the completeness of the R6G-D-mercury reaction and at the same time facilitates FRET between NAC-QDs and R6G-D-Hg. The reactions are carried out at pH 7 to meet the requirements for application in environmental and biological systems.

In practice, 100 μL of the R6G-D ethanol solution is adjusted to pH 7 by using phosphate buffer and diluted to 200 μL. Then 100 μL of mercury solution within 0–1000 μg L^{-1} or sample digests/solutions are added and vibrated for 5 min. 100 μL of NAC-QDs is immediately introduced and incubated for another 5 min, followed by recording the fluorescence spectra and deriving the fluorescence intensity ratio of F_{508}/F_{554}. The certified reference material is determined by using standard addition, while the water samples are detected by using calibration curve.

2.5. Cell culture, incubation and colorimetric imaging

The NAC-QDs/R6G-D sensing system is used for *in vitro* colorimetric imaging of mercury in Hela cells. The living Hela cells are maintained in a DMEM medium containing 10% fetal bovine serum, 100 units mL^{-1} penicillin and 100 mg mL^{-1} streptomycin. Cell culture is performed in a complete medium at 37 °C under 5% CO_2. Afterward, the cells are washed with phosphate-buffer (PBS) for twice to remove the residual DMEM medium and dead cells. The Hela cells are then allowed to incubate with NAC-QDs/R6G-D for 4 h at 37 °C and washed by PBS for twice, followed by further incubating with 0, 50, 100, 150, 200, and 250 μg L^{-1} of mercury (in PBS buffer) for another 30 min at 37 °C. After washing with PBS for three times, the Hela cells are fastened with glycerol mounting medium for facilitating colorimetric imaging recorded by an inverted fluorescent microscope.

3. Results and discussions

3.1. The sensing characteristics to mercury by the NAC-QDs/R6G-D FRET system

In the present study, N-acetyl-L-cysteine stabilized QDs (NAC-QDs) is chosen as FRET donor to a fluorescent R6G-D-mercury conjugate, the latter is formed by conjugating mercury with the non-fluorescent R6G derivative. In the absence of mercury, the NAC-QDs/R6G-D FRET pair gives rise to green fluorescence, while yellow-green emission is encountered when the R6G derivative conjugating with mercury and fluorescence resonance energy transfer takes place from NAC-QDs donor to R6G-D-Hg acceptor (Scheme 1). The decrease of green fluorescence of the donor and the increment of yellow-green fluorescence from the acceptor facilitates the ratiometric fluorescence detection of mercury. At the same time, this approach is feasible for colorimetric imaging of mercury in biological systems, e.g., live Hela cells in the present work.

NAC-QDs and R6G-D are both responsive to mercury. The N-acetyl-L-cysteine stabilized quantum dots give much brighter emission at ~510 nm than those of typical TGA/MPA stabilized quantum dots or dye-fluorophores (Zhao et al., 2010; Cao et al., 2010). There is a strong binding affinity between mercury and NAC

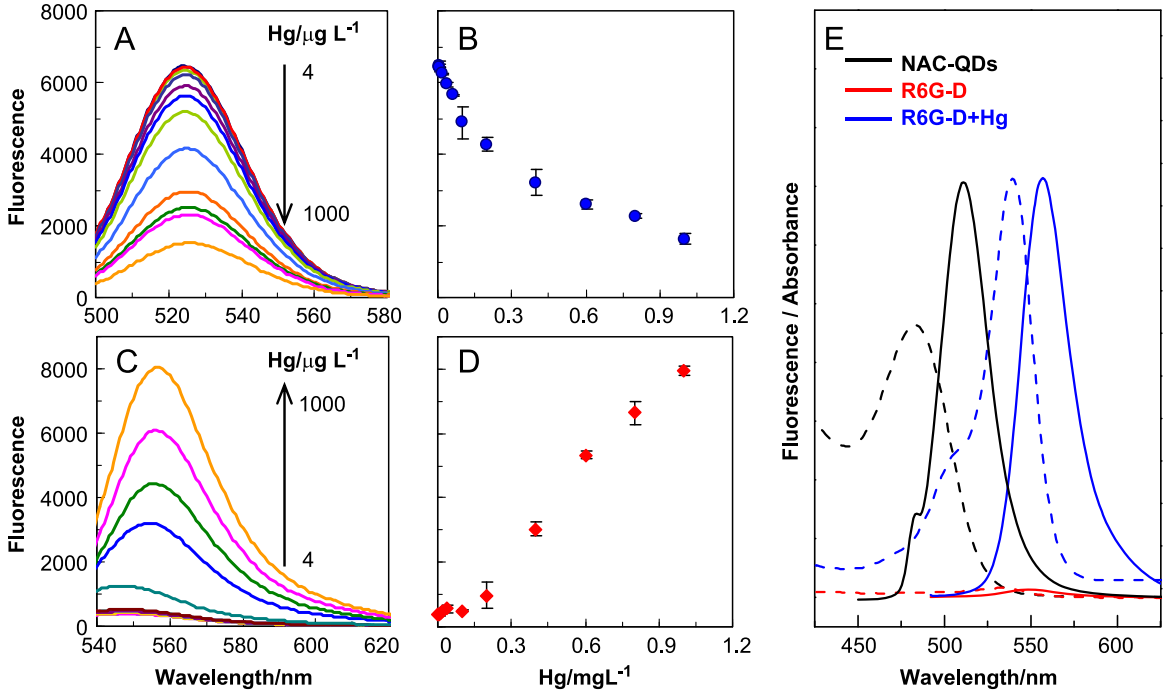

Fig. 1. The fluorescence response of NAC-QDs (spectrum A, curve B) and R6G-D (spectrum C, curve D) in the presence of mercury within a range of 4–1000 μg L^{-1}. NAC-QDs: 0.18 mmol L^{-1}; R6G-D: 6.6 μg mL^{-1}. (E) The fluorescence (solid lines) and absorption (dashed lines) spectra of NAC-QDs (black), R6G-D (red) and R6G-D-Hg conjugate (blue) in aqueous/ethanol suspension. (For interpretation of the references to color in this figure legend, the reader is referred to the web version of this article.)

moiety in the NAC-QDs, and thus mercury takes the NAC moiety away from the surface of quantum dots and form a more stable Hg–S bond, which results in decrease of the fluorescence of NAC-QDs. Fig. 1A and C illustrates obvious quenching of the fluorescence of NAC-QDs in the presence of mercury, and a linear relationship is achieved. It is imaginable that the selectivity of NAC-QDs is low because of similar interactions by other cationic and anionic species.

The conjugate between Rhodamine 6G derivative and mercury (R6G-D-Hg) exhibits high selectivity to the non-fluorescent enclosed spirolactam ring to facilitate the formation of fluorescent amide by ring-opening reaction (Dujols et al., 1997; Nguyen and Francis, 2003; Kwon et al., 2005). R6G-D itself is colorless and non-fluorescent (Wang et al., 2012), while the mercury-promoted desulfurization reaction and hydrolysis lead to a pink color and an obviously enhanced yellow-green fluorescence (Fig. 1B and D). This is attributed to the strong thiophilic affinity of mercury which releases thiosemicarbazide moiety with the mercury-facilitated ring opening of spirocycle group via coordination and drives the formation of 1,3,4-oxadiazole (Yang et al., 2005), which emits a strong yellow-green fluorescence.

Fig. 1E shows the emission and absorption spectra of NAC-QDs, R6G-D and R6G-D-Hg conjugate. It is seen that there is virtually no emission and absorption by R6G-D itself, but a strong absorption at $\lambda_{max}=535$ nm is observed for the R6G-D-Hg conjugate in the presence of mercury. This absorption spectrum has heavy overlap with the fluorescence spectrum of the donor NAC-QDs at $\lambda_{max}=508$ nm. This clearly indicates that excitation energy transfer could take place between NAC-QDs and R6G-D-Hg conjugate to give fluorescent emission at $\lambda_{max}=554$ nm. It is noteworthy that there is virtually no overlap between the maximum emission wavelength of NAC-QDs and R6G-D-Hg conjugate. This well facilitates the measurement of pure fluorescence intensities at $\lambda_{max}=508$ and 554 nm. On the other hand, R6G-D-Hg conjugate is an ideal acceptor with a large extinction coefficient of $4.5\times10^4\ M^{-1}\ cm^{-1}$, which could bring a high efficient resonance energy transfer. Förster radius R_0, the critical distance between donor and acceptor at a transfer efficiency of 50%, is expressed as follows (Lakowicz, 2006):

$$R_0^6 = 8.79\times10^{-25}K^2n^{-4}\varphi_x J$$

K^2 is the orientation factor related to the geometry of donor and acceptor of dipoles (2/3 for random orientation in solution), n is the average refract index of the medium, φ_x and J are the fluorescence quantum yield of donor and the effect of spectral overlap between the emission spectrum of donor and the absorption spectrum of acceptor, as calculated as follows (Rhodamine 6G as a reference with $\varphi_0=95\%$ in ethanol):

$$J=\frac{\int_0^\infty F(\lambda)\varepsilon(\lambda)\lambda^4\,d\lambda}{\int_0^\infty F(\lambda)\,d\lambda}$$

$$\phi_x=\phi_0\frac{F_x}{F_0}\frac{A_0}{A_x}\left(\frac{n_x}{n_0}\right)^2$$

J and φ_x are derived to be $5.93\times10^{-13}\ cm^3\ L\ mol^{-1}$ and 0.07 respectively. In turn, R_0 for the NAC-QDs and R6G-D-Hg FRET pair is derived to be 4.1 nm.

To further demonstrate the existence of FRET, the average distance r of the donor–acceptor pair is calculated according to a previous literature (Lakowicz and Maliwal, 1993). At a FRET efficiency of 66.4%, r is deduced to be 3.7 nm which is located in the 2–9 nm range.

The above discussions demonstrate that a novel ratiometric fluorescence sensing approach has been developed for the detection of mercury based on the NAC-QDs/R6G-D-Hg FRET ratiometric fluorescence protocol. The analytical performances of the sensing system can be seen from Fig. 2A. At low mercury concentration, the fluorescence of NAC-QDs decreases due to energy transfer and quenching effect. While at higher mercury concentration, the increase of resonance energy transfer efficiency causes a significant decrease of NAC-QDs fluorescence and a remarkable increment for the R6G-D-Hg conjugate fluorescence. The ratio of fluorescence intensity at the two maximum wavelengths, i.e., F_{508}/F_{554}, correlates closely to mercury concentration, providing the basis for quantitative analysis. A linear relationship is achieved within 5–250 μg L^{-1} as illustrated in Fig. 2B, with a regression equation of $F_{508}/F_{554}=-0.02454\ C_{Hg}$ (μg L^{-1})−8.2511. A detection limit of 0.75 μg L^{-1} (3σ/s, $n=11$) and a precision of 3.2% RSD are achieved at 175 μg L^{-1}.

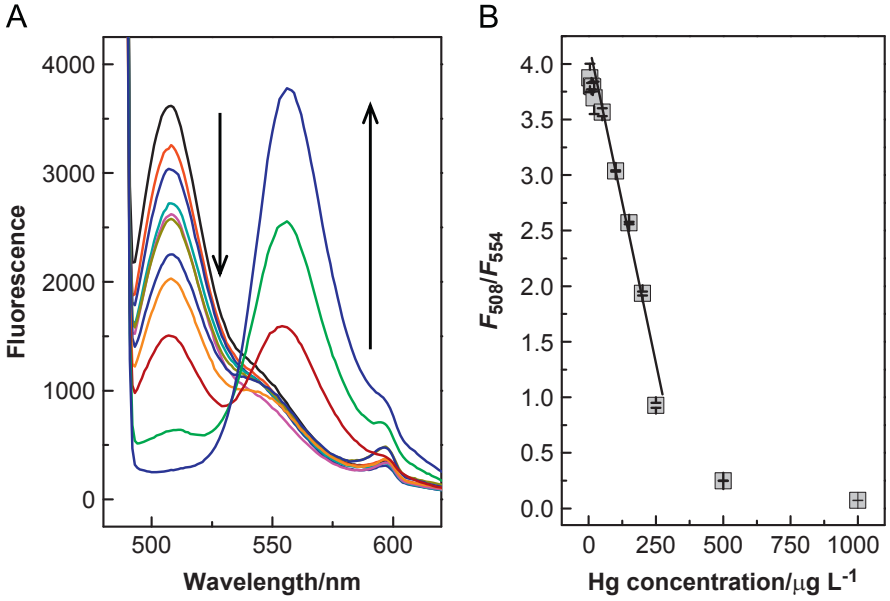

Fig. 2. (A) Fluorescence spectra of the NAC-QDs/R6G-D FRET assay system in the presence of various amounts of mercury (5, 10, 15, 20, 50, 100, 150, 200, 250, 500, and 1000 μg L^{-1}); (B) The linear calibration graph between F_{508}/F_{554} and the mercury concentration. NAC-QDs: 0.18 mmol L^{-1}; R6G-D: 6.6 μg mL^{-1}.

3.2. Selectivity of the sensing system

In order to demonstrate the practical applicability of the NAC-QDs/R6G-D-Hg FRET ratiometric fluorescence sensing system, potential interferences from various coexisting species frequently encountered in environmental and biological sample matrixes are investigated by conducting selectivity trials and competition experiments. The sensing system is excited at 490 nm and the fluorescence ratios of F_{508}/F_{554} for the competing ions are recorded in the absence (as a blank control) and presence of mercury. The results are given in Fig. 3A and B by evaluating the variation of the ratio $(F_{508}/F_{554})_{Hg}/(F_{508}/F_{554})_{control}$. It is obvious that in the selectivity trials, 0.2 mg L^{-1} of mercury causes a significant decrease on the F_{508}/F_{554} ratio, while 10 mg L^{-1} of common cations and anions give rise to virtually no change on F_{508}/F_{554}. When 0.2 mg L^{-1} of mercury is coexisting with 10 mg L^{-1} of the mentioned cations and anions, the F_{508}/F_{554} values remain unchanged with respect to that achieved for solely 0.2 mg L^{-1} mercury.

Mercury is a sulfophile metal with a very strong thiophilic affinity, it is essential to investigate the potential interfering effects from coexisting sulfophile elements, e.g., silver, copper, lead, cadmium and zinc. It indicated that although silver and copper are able to induce similar desulfurization reactions as that caused by mercury, the interferences from same amount of silver and copper on the sensing of mercury are not obvious (Fig. 3C-D). This observation is consistent with that of previous reports (Gong et al., 2012). In practical applications, silver and copper concentrations are often higher than that of mercury. Therefore, it is necessary to completely eliminate the potential interferences of these sulfophile metals. In this respect, the time-dependent fluorescence intensity ratio (F_{508}/F_{554}) of NAC-QDs, R6G-D and NAC-QDs/R6G-D sensing systems are evaluated for same amount of mercury, silver and copper. It is observed in Fig. 3E–G that F_{508}/F_{554} ratio approaches virtually a constant value at a suitably longer reaction time. For the NAC-QDs/R6G-D sensing system, a reaction time of 5 min is appropriate. In such a case, the NAC-QDs/R6G-D FRET ratiometric fluorescence protocol provides satisfactory selectivity for mercury sensing in the presence of coexisting cationic and anionic sample matrix components.

The variations of fluorescence intensity ratio F_{508}/F_{554} within 25 min are shown in Fig. S4a with 11 repetitive measurements in Fig. S4b. The virtually constant values well illustrate favorable stability for the NAC-QDs/R6G-D FRET sensor.

3.3. Mercury detection in a certified reference material and water samples

In order to demonstrate the practical applicability of the present FRET ratiometric fluorescence mercury assay system, mercury content in a certified reference material of CRM 176 is determined. It is obvious from Table 1 that fair agreement is achieved between the obtained concentration and the certified value for the CRM 176. In addition, spiking recoveries are performed for a series of environmental water samples, e.g., spring water, underground water and polluted water. It is evident that

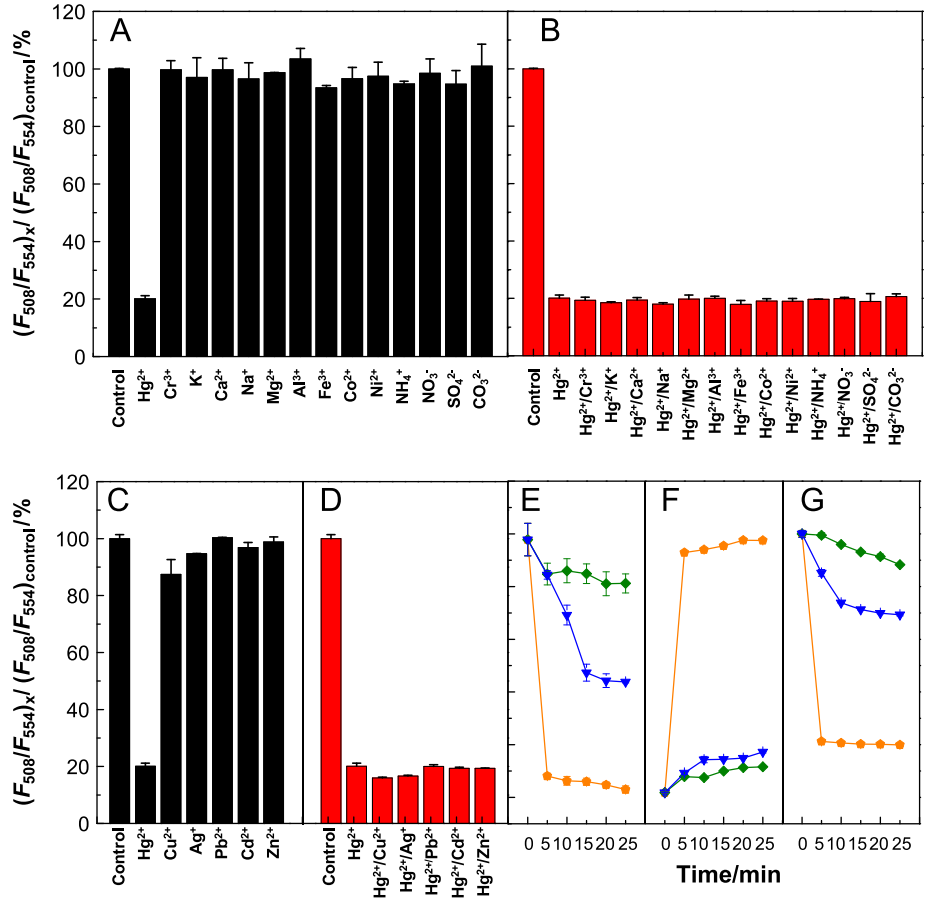

Fig. 3. The variation of fluorescence intensity ratio of F_{508}/F_{554} for the NAC-QDs/R6G-D FRET sensing system. (A) in the presence of 10 mg L^{-1} of coexisting common cations and anions, e.g., Cr^{3+}, K^+, Ca^{2+}, Na^+, Mg^{2+}, Al^{3+}, Fe^{3+}, Co^{2+}, Ni^+, NH_4^+, NO_3^-, SO_4^{2-} and CO_3^{2-}; (B) in the presence of 0.2 mg L^{-1} Hg^{2+} and 10 mg L^{-1} of the above cations and anions; (C) in the presence of 0.2 mg L^{-1} of sulfophile metals including Cu^{2+}, Ag^+, Pb^{2+}, Cd^{2+} and Zn^{2+}; (D) in the presence of 0.2 mg L^{-1} Hg^{2+} and 0.2 mg L^{-1} of the mentioned sulfophile metals; (E–G) the time-dependent fluorescence intensity ratio for NAC-QDs ($F_x/F_{control}$), R6G-D ($F_x/F_{control}$) and NAC-QDs/R6G-D $(F_{508}/F_{554})_x/(F_{508}/F_{554})_{control}$ with 0.2 mg L^{-1} Hg^{2+} (⬟), Cu^{2+} (▼) and Ag^+ (◆) respectively.

favorable spiking recoveries for mercury are achieved for these sample matrixes.

3.4. Visual detection of mercury and its colorimetric imaging in live cells

As discussed previously, in the absence of mercury, the NAC-QDs/R6G-D FRET ratiometric fluorescence sensing system exhibits brilliant yellow color under exposure of natural light, while it emits green fluorescence when excited by UV light at $\lambda_{ex}=365$ nm. The presence of mercury results in decrease of the green fluorescence from NAC-QDs, and at the same time it triggers the R6G-D to exhibit a pink color in visible light region, accompanying with a yellow-green fluorescent emission which is in association with mercury concentration. This indicates a gradual color change from green to yellow-green with the increase of mercury concentration, and thus provides a possibility for visual detection of mercury as well as its colorimetric imaging. Fig. 4A clearly illustrates the fluorescence chromatic difference imaging of mercury. It is seen that visual detection of mercury is feasible within a range of 0–250 μg L^{-1}, and a visual distinguishing ability for the sensing of mercury is *ca.* 50 μg L^{-1}.

A further study has been performed to demonstrate colorimetric imaging of intracellular mercury in live cells by use of the present NAC-QDs/R6G-D FRET ratiometric fluorescence system. The Hela cells used for this purpose are cultured and treated as described in the Experimental section. Fig. 4B shows the fluorescence images of living Hela cells. It is seen that a weak green fluorescence is observed when Hela cells are incubated with bare NAC-QDs/R6G-D for 4 h. This indicates that both NAC-QDs and R6G-D exist in the cells and spirolactam structure of R6G-D is maintained (Tang et al., 2008; Shamsipur et al., 2005). When the Hela cells pre-incubated with NAC-QDs/R6G-D are further incubated in the presence of mercury, a R6G-D-Hg conjugate is formed and its fluorescence is observed, as illustrated by the fact that the fluorescent emission color of the Hela cells is progressively changed from green to yellow-green with the increase of mercury

Table 1
The determination of mercury in a certified reference material CRM 176 and three environmental water samples ($n=3$, 95% confidence level).

Sample	Standard (μg g^{-1})	Found (μg L^{-1})	Spiked (μg L^{-1})	Recovered[b] (μg L^{-1})	Recovery[b] (%)
CRM 176	31.4 ± 1.1	31.3 ± 1.6[a]			
Spring water		< LOD	20	20.08 ± 0.45	100.4 ± 2.2
Underground water		< LOD	20	20.27 ± 0.18	101.4 ± 0.9
Polluted water		< LOD	20	19.30 ± 0.45	95.5 ± 2.2

[a] Standard addition method (μg g^{-1}), $n=3$, means $\pm t\cdot s/\sqrt{n}$, $f=95\%$, $t=4.303$.
[b] Standard curve method, $n=2$, means $\pm t\cdot s/\sqrt{n}$, $f=95\%$, $t=12.706$.

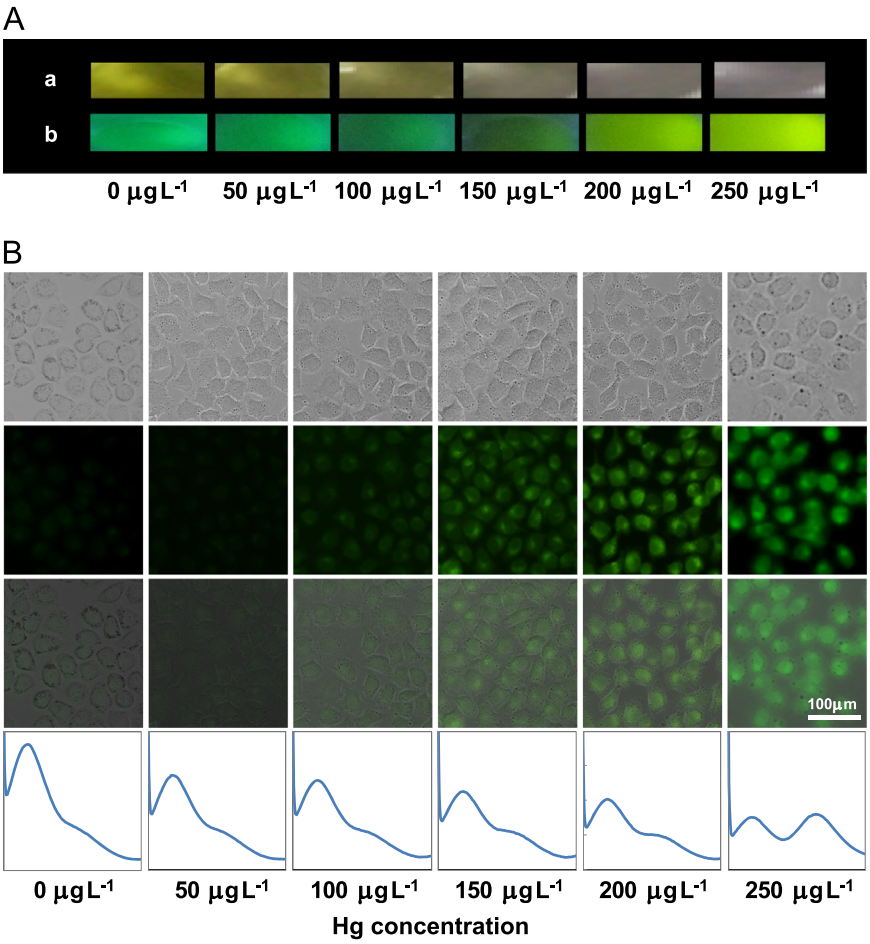

Fig. 4. (A) Colorimetric images of mercury in the range of 0–250 μg L^{-1} under (a) natural light and (b) UV light at λ_{ex} 365 nm. (B) Images of Hela cells incubated by NAC-QDs/R6G-D for 4 h and further treated at different levels of mercury (0, 50, 100, 150, 200, and 250 μg mL^{-1}) for 30 min. (row 1: bright-field images; row 2: fluorescence images; row 3: merged images of the birght-feild and fluorescence images; row 4: fluorescence spectra at various mercury concentrations). NAC-QDs: 0.01 mmol L^{-1}; R6G-D: 2.0 μg mL^{-1}; the excitation and emission are centered at 495 ± 10 nm and 520 ± 10 nm, respectively.

concentration. These observations indicate that the NAC-QDs/R6G-D FRET ratiometric fluorescence sensing system is feasible for quantitative colorimetric imaging of intracellular mercury.

4. Conclusions

Ratiometric mercury sensor based on fluorescence resonance energy transfer (FRET) from N-acetyl-L-cysteine stabilized quantum dots (NAC-QDs) to Rhodamine 6G derivative-mercury conjugate (R6G-D-Hg) has the features for sensitive and selective measurement of mercury as well as its visual detection by colorimetric imaging. This has been further demonstrated by intracellular imaging of mercury. In addition, by performing measurement with a two-wavelength mode at the maximum fluorescent wavelength of NAC-QDs and R6G-D-Hg conjugate, the spurious factors and the fluorescence fluctuations are effectively eliminated. The observations in the present study provide an approach for further development of ratiometric sensors dedicated to selective *in vitro* or *in vivo* sensing of biologically interest species.

Acknowledgment

Financial support from Natural Science Foundation of China (21275027, 21235001, and 21075013), the Program of New Century Excellent Talents in University (NCET-11–0071) and Fundamental Research Funds for the Central Universities (N110705002, N120605002, and N110805001) are appreciated.

Appendix A. Supporting information

Supplementary data associated with this article can be found in the online version at http://dx.doi.org/10.1016/j.bios.2013.06.004.

References

Boening, D.W., 2000. Chemosphere 40, 1335–1351.
Cao, J., Xue, B., Li, Hui, Deng, D.W., Gu, Y.Q., 2010. Journal of Colloid and Interface Science 348, 369–376.
Chatterjee, A., Santra, M., Won, N., Kim, S., Kim, J.K., Bin Kim, S., Ahn, K.H., 2009. Journal of the American Chemical Society 131, 2040.
Childress, E.S., Roberts, C.A., Sherwood, D.Y., LeGuyader, C.L.M., Harbron, E.J., 2012. Analytical Chemistry 84 (3), 1235–1239.
Darbha, G.K., Ray, A., Ray, P.C., 2007. ACS Nano 1, 208–214.
da Silva, D.G., Portugal, L.A., Serra, A.M., Ferreira, S.L.C., Cerdà, V., 2013. Food Chemistry 137, 159–163.
Duan, J.L., Jiang, X.C., Ni, S.Q., Yang, M., Zhan, J.H., 2011. Talanta 85, 1738–1743.
Dujols, V., Ford, F., Czarnik, A.W., 1997. Journal of the American Chemical Society 119, 7386–7387.
Erxleben, H., Ruzicka, J., 2005. Analytical Chemistry 77, 5124–5128.
Fang, C., Zhao, B.M., Lu, H.T., Sai, L.M., Fan, Q.L., Wang, L.H., Huang, W., 2008. The Journal of Physical Chemistry C 112, 7278–7283.
Geng, W.H., Nakajima, T., Takanashi, H., Ohki., A., 2008. Journal of Hazardous Materials 154, 325–330.
Gong, Y.J., Zhang, X.B., Chen, Z., Yuan, Y., Jin, Z., Mei, L., Zhang, J., Tan, W.H., Shen, G.L., Yu, R.Q., 2012. Analyst 137, 932–938.
Han, S., Narasingarao, P., Obraztsova, A., Gieskes, J., Hartmann, A.C., Tebo, B.M., Allen, E.E., Deheyn, D.D., 2010. Environmental Science and Technology 44, 3752–3757.
Hu, B., Zhang, L.P., Chen, M.L., Chen, M.L., Wang, J.H., 2012. Biosensors and Bioelectronics 32 (1), 82–88.
Hight, S.C., Cheng, J., 2006. Analytica Chimica Acta 567 (2), 160–172.
Kenmoku, S., Urano, Y., Kojima, H., Nagano, T., 2007. Journal of the American Chemical Society 129, 7313–7318.
Kim, H.J., Lee, S.J., Park, S.Y., Jung, J.H., Kim, J.S., 2008. Advanced Materials 20, 3229.
Kim, H.N., Nam, S.W., Swamy, K.M.K., Jin, Y., Chen, X.Q., Kim, Y., Kim, S.J., Park, S., Yoon, J., 2011. Analyst 136, 1339–1343.
Kwon, J.Y., Jang, Y.J., Lee, Y.J., Kim, K.M., Seo, M.S., Nam, W., Yoon, J., 2005. Journal of the American Chemical Society 127, 10107–10111.
Lakowicz, J.R., Maliwal, B., 1993. Analytica Chimica Acta 271, 155–164.
Lakowicz, J.R., 2006. Principles of Fluorescence Spectroscopy, 3rd ed. Kluwer Academic/Plenum, New York, pp. 443–447.
Leermakers, M., Baeyens, W., Quevauviller, P., Horvat, M., 2005. TrAC Trends in Analytical Chemistry 24, 383–393.
Leopolda, K., Harwardt, L., Schustera, M., Schlemmer, G., 2008. Talanta 76, 382–388.
Li, H.L., Fan, J.L., Wang, J.Y., Tian, M.Z., Du, J.J., Sun, S.G., Sun, P.P., Peng, X.J., 2009. Chemical Communications, 5904–5906.
Li, H.L., Fan, J.L., Du, J.J., Guo, K.X., Sun, S.G., Liu, X.J., Peng, X.J., 2010. Chemical Communications 46, 1079–1081.
Ma, Q., Su, X.G., Wang, X.Y., Wan, Y., Wang, C.L., Yang, B., Jin, Q.H., 2005. Talanta 67, 1029–1034.
Magos, L., Clarkson, T.W., 2006. Annals of Clinical Biochemistry 43, 257–268.
Mutter, J., Naumann, J., Schneider, R., Walach, H., Haley, B., 2005. Neuroendocrinology Letters 26, 439–446.
Nguyen, T., Francis, M.B., 2003. Organic Letters 5, 3245–3248.
Nolan, E.M., Lippard, S.J., 2008. Chemical Reviews 108, 3443–3480.
Pei, J.Y., Zhu, H., Wang, X.L., Zhang, H.C., Yang, X.R., 2012. Analytica Chimica Acta 757, 63–68.
Pourreza, N., Ghanemi, K., 2009. Journal of Hazardous Materials 161, 982–987.
Shamsipur, M., Hosseini, M., Alizadeh, K., Alizadeh, N., Yari, A., Caltagirone, C., Lippolis, V., 2005. Analytica Chimica Acta 533, 17–24.
Swamy, K.M.K., Ko, S.K., Kwon, S.K., Lee, H.N., Mao, C., Kim, J.M., Lee, K.H., Kim, J., Shin, I., Yoon, J., 2008. Chemical Communications, 5915–5917.
Tang, B., Cui, L.J., Xu, K.H., Tong, L.L., Yang, G.W., An, L.G., 2008. ChemBioChem 9, 1159–1164.
Tchounwou, P.B., Ayensu, W.K., Ninashvili, N., Sutton, D., 2003. Environmental Toxicology 18, 149–175.
Tsay, J.M., Trozoss, M., Shi, L.X., Kong, X.X., Selke, M., Jung, M.E., Weiss, S., 2007. Journal of the American Chemical Society 129, 6865–6871.
Wang, L.N., Yan, J.X., Qin, W.W., Liu, W.S., Wang, R., 2012. Dyes and Pigments 92, 1083–1090.
Xiang, Y., Tong, A., 2006. Organic Letters 8, 1549–1554.
Xiang, Y., Tong, A., Jin, P., Ju, Y., 2006. Organic Letters 8, 2863–2866.
Yang, X.R., Liu, H.X., Xu, J., Tang, X.M., Huang, H., Tian, D.B., 2011. Nanotechnology 22, 275503–275518.
Yang, Y.K., Yook, K.J., Tae, J., 2005. Journal of the American Chemical Society 127, 16760–16761.
Yin, Y.M., Liang, J., Yang, L.M., Wang., Q.Q., 2007. Journal of Analytical Atomic Spectrometry 22 (3), 330–334.
Zahir, F., Rizwi, S.J., Haq, S.K., Khan, R.H., 2005. Environmental Toxicology and Pharmacology 20, 351–360.
Zhao, D., He, Z.K., Chan, P.S., Wong, R.N.S., Mak, N.K., Lee, A.W.M., Chan, W.H., 2010. The Journal of Physical Chemistry C 114, 6216–6221.